MECHANICAL BEHAVIOR OF A 2D SiC/SiC COMPOSITE WITH A MULTILAYERED MATRIX

P. Forio, J. Lamon

Laboratoire des Composites Thermostructuraux
UMR 5801 (CNRS-SNECMA/SEP-UB1-CEA)
3, Allée de la Boétie, 33600 Pessac, France

SUMMARY: The mechanical behavior of a new generation of 2D Nicalon/SiC composite with a multilayered matrix, made by chemical vapor infiltration (CVI), has been investigated under tensile loading at room temperature. Damage was observed on the specimens under load using an optical microscope. Acoustic emission was analysed in terms of number of counts, amplitude distribution, and number of events.
The influence of the microstructure and of pre-existing cracks was determined. Comparison of damage observations with acoustic emission data and the mechanical behavior showed that matrix cracking is the preponderant damage mechanism, and allowed the contribution of crack families to be evaluated.

KEYWORDS: 2D SiC/SiC composite, multilayered matrix, damage, acoustic emission.

INTRODUCTION

The ceramic matrix composites reinforced with long fibers are potential materials in aerospace industry, for use in severe conditions of temperature and environment. For instance, the SiC/SiC composites consisting of a SiC matrix reinforced by SiC fibers display some favorable characteristics such as high mechanical properties and a good resistance to high temperature.

It is well acknowledged that the properties of fiber/matrix interfaces determine the mechanical behavior of brittle-matrix composites [1,2]. Pyrocarbon has proven to be the most-efficient interphase to control fiber/matrix interactions and the composite mechanical behavior. But, pyrocarbon is sensitive to oxidation at temperatures>500°C. To protect this interphase from oxidation, multilayered composites have been developed, first with a SiC matrix and a multilayered interphase consisting of alternate SiC and PyC sublayers [3,4], and more recently with a multilayered matrix [5]. The main goal of multilayering the matrix is to introduce phases which produce sealants at high temperature that heal the matrix cracks and prevent the oxygen from reaching the interphase.

In the composites reinforced with fabrics of fiber tows, the matrix damage is influenced by the microstructure. The 2D SiC/SiC composites made by chemical vapor infiltration (CVI) of a fiber preform display a heterogeneous microstructure consisting of woven infiltrated tows that behave as physical entities, large pores (referred to as macropores) located between the plies or at yarn intersections, and a uniform layer of matrix over the fiber preform (the intertow matrix). Extensive inspection of 2D SiC/SiC composites under a tensile load, using a microscope, has shown that matrix cracking affects first the intertow matrix, then the transverse infiltrated tows and finally the longitudinal tows [6]. A comparable three stage matrix cracking has been identified in a SiC/SiBC composite with a multilayered matrix [5]. The work reported in the present paper was aimed at investigating the influence of damage

and matrix cracking on the mechanical behavior of a new generation of 2D SiC/SiC composites with a multilayered matrix. Optical microscopy and acoustic emission techniques were employed for the detection and analysis of damage mechanisms.

MATERIALS

The 2D SiC/SiC composite investigated in the present paper consists of a woven preform of treated tows of Nicalon fibers* coated with a pyrocarbon thin layer as interphase and embedded in a multilayered matrix. Both the interphase and the matrix were deposited by CVI (fig. 1). The matrix is essentially composed of three elements: Si, B, C. Two batches (a, b) of this composite have been tested. The main characteristics of the materials are given in table 1. The Young modulus of the multilayered matrix was estimated from the mixture's rule.

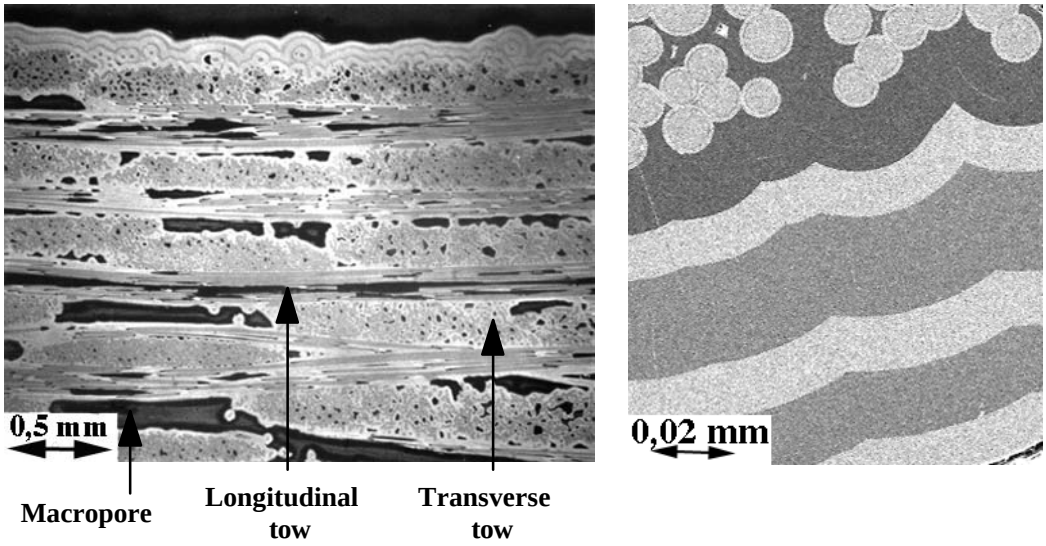

Fig. 1: Micrographs showing the microstructure of the 2D SiC/SiC composite with a multilayered matrix.

The as-received specimens contained pre-existing cracks which were located in the matrix, parallel to the interface between two layers. These longitudinal cracks were detected in the thickest sublayer near the surface (type I cracks) (fig. 2). In the specimens from batch b, additionnal pre-existing longitudinal cracks were observed in thin SiC layers in the interior of specimens (type II cracks) (fig. 3).

Batch	V_f (%)	V_p (%)	Matrix	E_m (GPa)	E_f (GPa)	Type of Pre-existing crack
a	40	12	9 layers	290	200	I
b	40	12	10 layers	290	200	I + II

Table 1: Main characteristics of the 2D SiC/SiC composites with a multilayered matrix.

(* proprietary treatment, SEP, division de SNECMA)

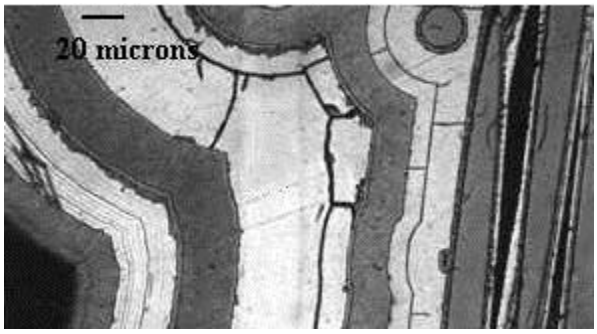

Fig. 2: Pre-existing matrix cracks located in a thick sublayer (type I)

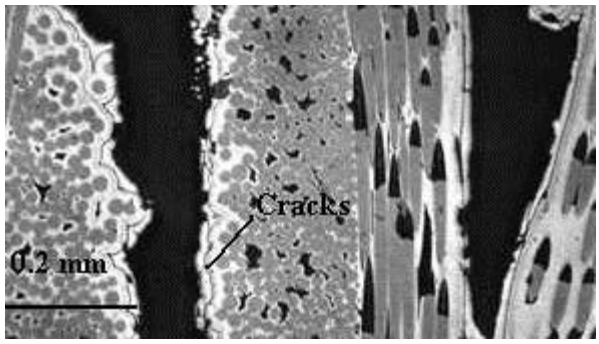

Fig. 3: Pre-existing matrix cracks located in a thin SiC sublayer (type II)

EXPERIMENTAL

The tensile tests were performed at room temperature with a constant cross-head displacement rate of 0.05mm/min. Some specimens were polished to allow observation of damage under load using an optical microscope. Inspection of the surface of specimens was conducted at the following strain levels : 0.08%, 0.10%, 0.15%, 0.20%, 0.25%, 0.30%, 0.40%. The images were recorded with a digital camera and stored on disks using a PC. Two specimen geometries were used (table 2).

The deformations were measured using an extensometer. The gauge length is given in table 2. Unloading-reloading cycles were carried out, in order to estimate the residual strains at zero load, the fiber/matrix bonding, and the elastic modulus at various stages of damage. The elastic modulus was derived from the slope of the stress-strain curve on reloading.

Batch	Specimen	Specimen dimensions	Gauge length
a	**1**	**16 mm x 4.5 mm x 150 mm**	**25 mm**
b	**2**	**10 mm x 4.5 mm x 70 mm**	**10 mm**
b	**3**	**10 mm x 4.5 mm x 70 mm**	**10 mm**
b	**4**	**16 mm x 4.5 mm x 150 mm**	**25 mm**

Table 2: Specimen dimensions.

After ultimate failure, the broken test specimens were examined by Scanning Electron Microscopy and by Optical Microscopy.

Acoustic emission was monitored using a transducer positioned on the specimen, with silicon oil as coupling. The acoustic emission signals were recorded and processed with an acoustic emission LOCAN 320 equipment. The waveforms and their frequency spectra were acquired using a digital oscilloscope. The piezo electric transducer (PAC Micro 30) and the 40 dB fixed gain preamplifier have the same wide band frequency (100-300KHz).

RESULTS AND DISCUSSION

Mechanical properties.

The tensile stress-strain curves (σ-ε) (fig. 4) exhibit a non-linear domain beyond the proportional limit indicating a non-brittle mechanical behavior. The main features of the mechanical behavior are summarized in table 3. Comparable stress-strain curves were obtained for specimens 2, 3 and 4, showing that specimen geometry has no significant influence on the stress-strain behavior (no size effect). Furthermore, it is seen that the larger stresses and strains were obtained for the specimen of batch a. No linear domain is observed prior to ultimate failure, suggesting that the stage of matrix cracking was not saturated.

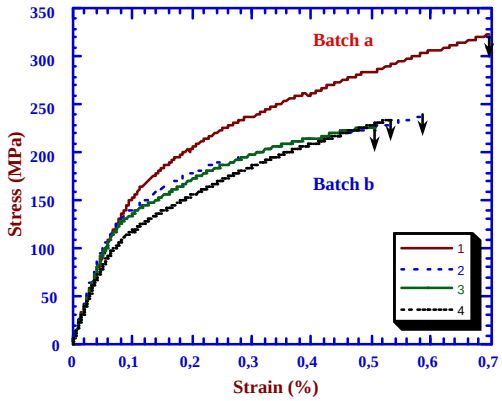

Fig. 4: Stress-strain behavior of the 2D SiC/SiC composites with a multilayered matrix.

Batch	Young Modulus E_0 (GPa)	Proportional limit ε_e (%)	σ_e (MPa)	Failure ε_r (%)	σ_r (MPa)
a	**189**	**0,039**	**75**	**0,69**	**324**
b	**196 [13,5]**	**0,035 [0,008]**	**69 [19]**	**0,53 [0,04]**	**232 [7,7]**

Table 3: Mechanical properties of 2D SiC/SiC composites.

Figure 5 shows the relative elastic moduli E/Eo (Eo is the initial elastic modulus of the composite), that have been measured during the tensile tests. The modulus decreases steeply to a minimum value of E/Eo = 0,26. This minimum is larger than the limit $0.5.E_f.V_f/Eo = 0.21$ (E_f is the fiber Young modulus, V_f the volume fiber fraction), which is reached when the load is carried only by the longitudinal fibers. This implies that the fibers were not completely debonded, that saturation of matrix cracking was not reached, and that individual fiber breaks did not occur. The modulus decrease is more substantial for batch b than for batch a. This suggests that damage including matrix cracking and debonding was more significant in batch b.

The residual strain at zero load is proportional to the applied deformation beyond the elastic domain. The residual strains are larger for specimens of batch b than for those of batch a (fig. 6).

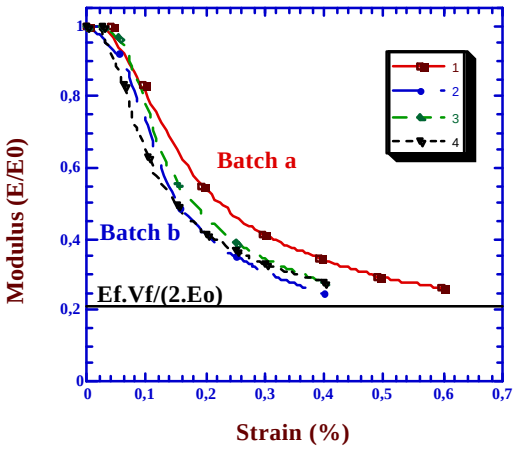

Fig. 5: Relative elastic modulus vs applied deformation during the deformation. tensile tests.

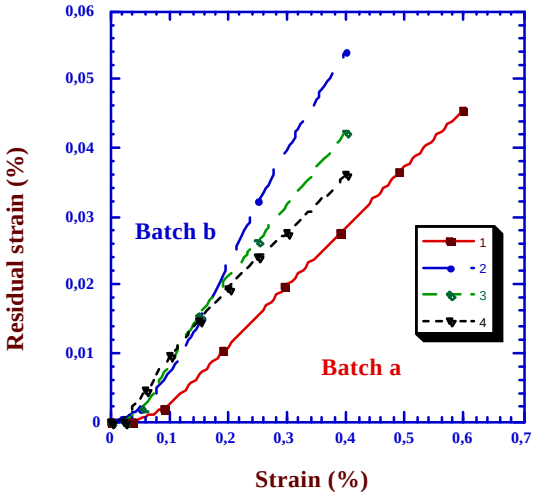

Fig. 6: Evolution of residual strain at zero load vs applied

Fiber/matrix bond.

The interfacial shear stress (τ) was estimated from the area of the hysteresis loops measured during the unloading-reloading cycles (eqn 1) [7]:

$$\tau_p = \frac{b_2.(1-a_1.V_f)^2.R_f}{12.E_m.l_s.V_f^2}.\frac{\sigma_p^3}{S} \qquad \text{(eqn 1)}$$

where l_s is the average spacing distance of matrix cracks, R_f is the fiber radius (7 µm), a_1 and b_2 Hutchinson and Jensen coefficients [7], S the area of unloading-reloading cycle, and σ_p the maximum stress of the cycle.

The average spacing distance (l_s), ranged between 15 µm and 27 µm along the longitudinal tows. It was measured on the broken specimens. The local volume fiber fraction within the longitudinal tows is 40%.

The interfacial shear stress is commensurate with the intensity of the fiber/matrix bond (table 4).

Batch	Specimen	Crack spacing distance l_s (µm)	Cycle area S (KJ/m^3)	Interfacial shear stress (eqn 1) τ_p (MPa)
a	1	15	54,5	203
b	3	27	33	64

Table 4: Interfacial shear stress estimation

The interfacial shear stress pertinent to batch a is three times as large as that of batch b. This discrepancy is consistent with the trend in modulus decrease which suggested longer debonds in specimens of batch b.

τ = 203 MPa obtained for the specimen of batch a is identical to that determined for conventional 2D SiC/SiC reinforced also with treated Nicalon fibers [8]. Therefore, this τ measurement may be regarded as satisfactory. The value obtained for specimens of batch b appears to be surprisingly by small since these specimens are also reinforced with treated Nicalon fibers.

Observation of matrix damage during loading.

The pre-existing crack families in the as-received specimens have been described above. Figure 7 summarizes the stress induced matrix damage evolution for batches a, and b, and for conventionnal 2D SiC/SiC composites [6].

Matrix damage in batch a is comparable to that observed in conventional 2D SiC/SiC: for strains < 0.10%, transverse cracks in the intertow matrix (A), for strains between 0.10% and 0.25%, cracks in the transverse tows (B), then for strains larger than 0.25%, multiple cracks in the longitudinal tows (C).

In those specimens of batch b, the transverse cracks which initiated in the intertow matrix (A) are arrested in a first step (at a deformation = 0.08%) by the pre-existing longitudinal type II cracks (fig. 8). In a second step (for strains between 0.10% and 0.20%), these cracks propagate to the longitudinal tows. Saturation of intertow matrix cracking is observed for a deformation of 0.20%. Cracking in the transverse tows is observed at deformations between 0.15% and 0.25% (B), and finally multiple cracking in the longitudinal tows starts at a strain around 0.25%. Cracks in the transverse tows seem to appear later in batch b (0.15%) than in batch a (0.10%), but, in both cases, this damage ends at the same strain, when multiple cracking in the longitudinal tows begins (0.25%). Figures 9 and 10 illustrate the deviation of transverse cracks by the longitudinal type II cracks.

A contribution of the type II longitudinal cracks to the hysteretic behavior may be expected, leading to smaller τ values, and more significant modulus decreases, when comparing with the specimen of batch a.

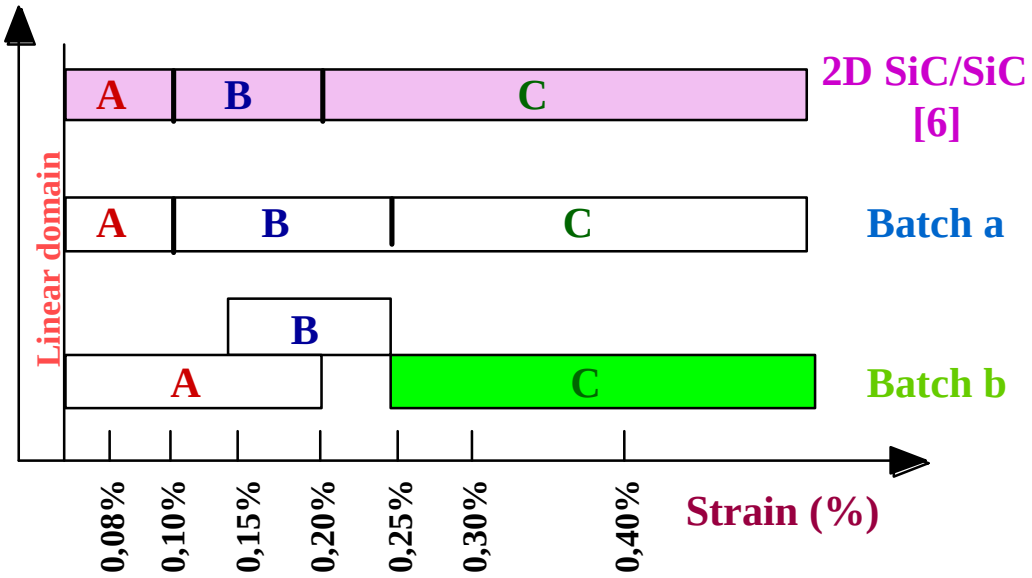

Fig. 7: Different matrix damage stages in 2D SiC/SiC composites.
(A, B, and C are depicted in figure 8)

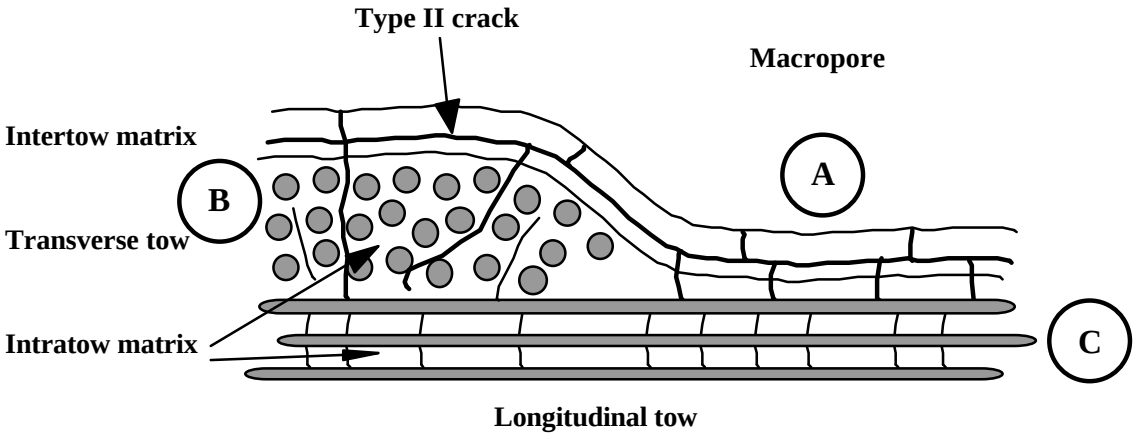

Fig. 8: Matrix damage modes identified in batch b.

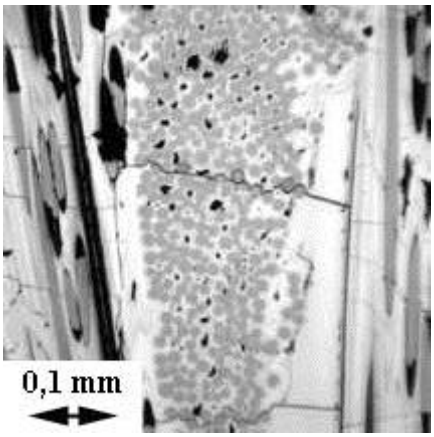

Fig. 9: Micrograph showing crack deviation by a longitudinal type II crack (specimen 3 at a strain = 0.40%)

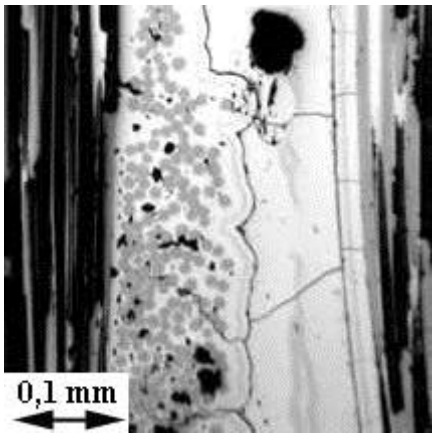

Fig. 10: Micrograph showing crack deviation by a longitudinal type II crack (specimen 4 at a strain = 0.40%)

Identification of damage using acoustic emission.

Figure 11 shows the different regimes of acoustic emission that can be detected during loading of a specimen of batch b:

no emission for strains below 0.025%.
an increasing activity for strains increasing from 0.025% to 0.08%.
an maximum rate of activity for strains between 0.08% and 0.12%.
and a continuously slowing down activity for strains larger than 0.12%.

The maximum rate of activity coincides with the first step of cracking, during which cracks appear in the intertow matrix and then are arrested by the longitudinal pre-existing cracks. The acoustic activity appears to mimic the trend in modulus decrease (fig. 5). The maximum rate of acoustic emission corresponds to the steepest modulus decrease. They reflect both the most damaging phenomenon. Then, as the activity slows down the modulus decrease becomes less substantial, indicating that damage becomes less significant.

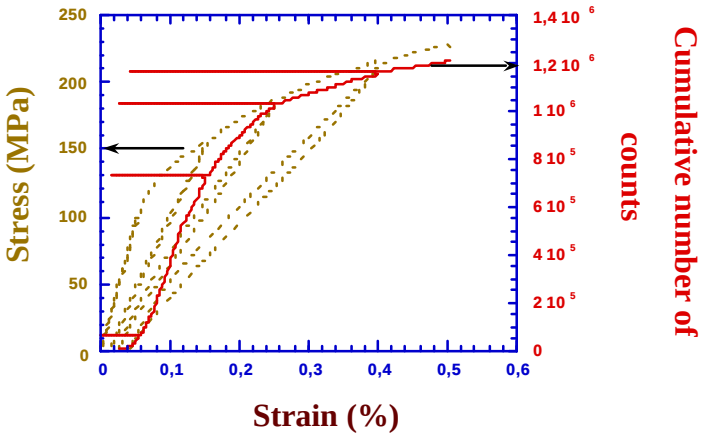

Fig. 11: Cumulative number of counts during a tensile test (specimen 3).

This trend is confirmed by the plot of count rate (fig. 12) which reveals a peak for an applied deformation of around 0.1%. This figure also shows that the count rate for specimen 4 is 3.4 times as high as that for specimen 3. This ratio corresponds to the ratio of stressed volume (3.6), suggesting that the activity is proportional to the density of cracks, and that the cracks are uniformly distributed over the specimen volume. A small peak was also detected at the end of the last unloading cycle. This peak may be related to the microbuckling of the debonded fibers indicated by the stiffening of the stress-strain curve at the end of unloading. It suggests that a certain damage is associated to microbuckling.

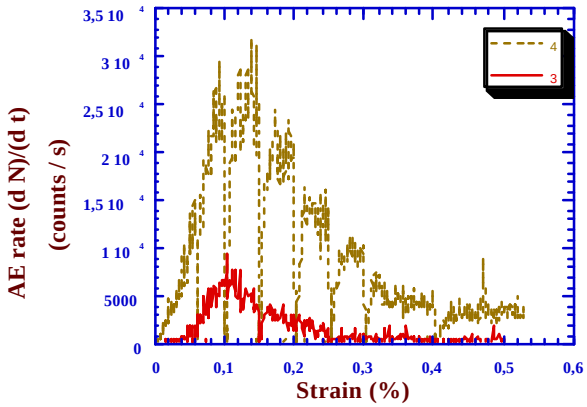

Fig. 12: Acoustic emission rate vs applied deformation.

The distributions of amplitudes seem to involve a single population of events (fig. 13). However at a deformation of 0.03%, when matrix cracking and debonding dominate (fiber breaks and associated pull-out cannot occur at such low deformation), two distinct populations of events can be identified: the first one for the amplitudes ranging between 36 and 52 dB, and the second one for the amplitudes between 53 and 59 dB.

It has been established that the failures of Nicalon fibers produce events above 65 dB [9]. These populations of events are in agreement with the results of a previous study on acoustic events in 2D SiC/SiC composites [10], that indicated that the amplitude distribution can be subdivided into four families corresponding to the damage phenomena: 35-50 dB (matrix cracking), 51-60 dB (debonding), 60-70 dB (pull-out) and 70-100 dB (fiber failures). Figure 14 shows a plot of the respective numbers of acoustic events associated to the above mentionned families of amplitude. It can be seen that the largest numbers of events are obtained for the amplitudes attributed to matrix cracking. Comparatively low numbers of events are obtained for the other phenomena. It is worth mentioning that the number of events pertinent to fiber failures is quite negligible. This results is in agreement with the literature

[11], which showed that individual fiber breaks are limited and occur only at high stresses near the ultimate failure in SiC/SiC composites.

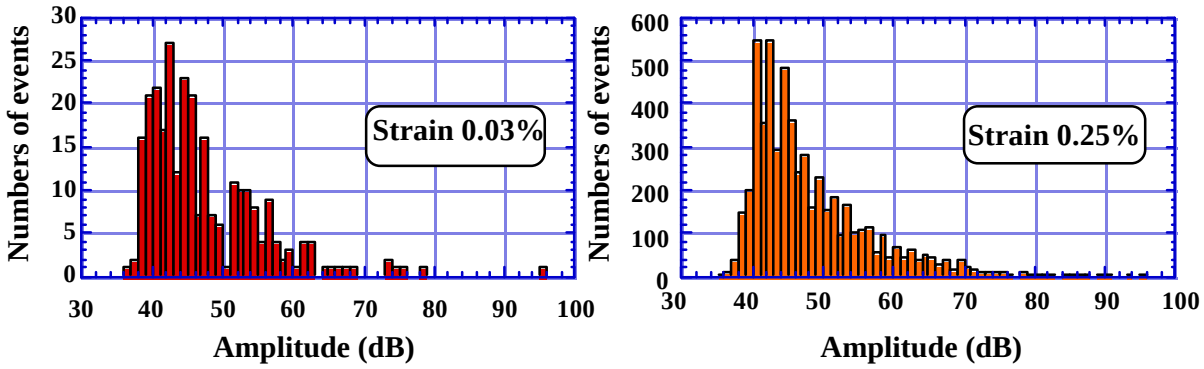

Fig. 13: The distributions of event amplitudes at deformations 0.03% and 0.25%.

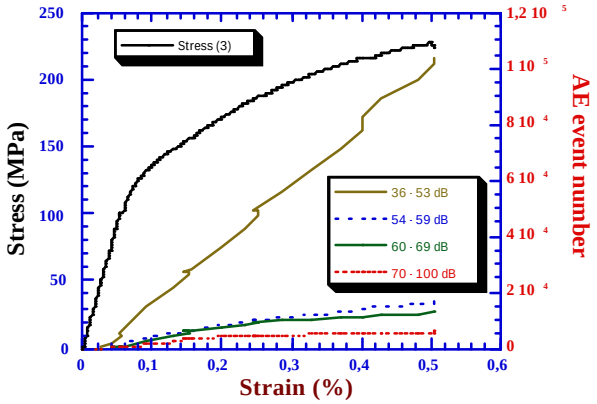

Fig. 14: Evolution of the four families of AE events, during a tensile test.

CONCLUSION

The stress-strain behavior of a new generation of 2D SiC/SiC composites with a multilayered matrix was investigated with respect to the damage identified by in-situ microscopy and acoustic emission.

The stress-strain behavior and the damage mechanisms appeared to be influenced by the microstructure. The matrix damage involves essentially three families of cracks located in the intertow matrix, in the transverse tows and in the longitudinal tows. However, some differences with the conventional 2D SiC/SiC composites were found. Furthermore, the pre-existing longitudinal cracks detected in specimens of batch b, appeared to favor deviation of the cracks propagating in the intertow matrix.

The analysis of acoustic emission data confirmed the trends evidenced by microscopy. It allowed the contribution of the different crack families to the mechanical behavior to be evaluated. The first family of intertow matrix cracks appeared to be the most damaging. It was confirmed that matrix cracking is the preponderant damage mechanism, fiber pull-out and individual fiber breaks exert a comparatively limited influence on the mechanical behavior.

Data and knowledge on the mechanical behavior of a new generation of 2D SiC/SiC composites with a multilayered matrix were generated. It was also shown that optical microscopy and analysis of acoustic emission data are complementary tools to investigate the relationships between the mechanical behavior and damage in CMCs.

Acknowledgement.

This work has been supported by SEP and CNRS through a grant given to P. F. The authors acknowledge E. Pestourie for available discussion, SEP, division de SNECMA for the processing of the samples, and B. Humez for mechanical tests.

References.

1. Evans, A.G., and Marshall, D.B., "The Mechanical Behavior of Ceramic Matrix Composites", Acta Met., Vol. 37, No. 10, 1989, pp. 2567-2583.

2. Kerans, R.J., Hay, R.S., Pagano, N.J., and Parthasarathy, T.A., "The Role of the Fiber-Matrix Interface in Ceramic Matrix Composites", Am. Ceram. Soc. Bull., Vol. 68, No. 2, 1988, pp. 429-442.

3. Bertrand, S., Forio, P., Pailler, R., and Lamon, J., "Hi-Nicalon/SiC Minicomposites with (PyC/SiC)n Nanoscale Multilayered Interphase", J. Am. Ceram. Soc., in press.

4. Droillard, C., and Lamon, J., "Fracture Toughness of 2-D Woven SiC/SiC CVI-Composites with Multilayered Interphases", J. Am. Ceram. Soc., Vol. 79, No. 4, 1996, pp. 849-858.

5. Carrère, P., "Thermostructural Behavior of a SiC/SiC Composite", PhD thesis n° 1592, 1996, University of Bordeaux I.

6. Guillaumat, L., Lamon, J., "Multicracking of SiC/SiC Composites", Revue des Composites et des Matériaux Avancés, Vol. 3, No. hors série, 1993, pp. 159-171 (in French).

7. Lamon, J., Rebillat, F., Evans, A.G., "Microcomposite Test Procedure for Evaluating the Interface Properties of Ceramic Matrix Composites" J. Am. Ceram. Soc., Vol. 78, No. , 1995, pp. 401-405.

8. Droillard, C., Voisard, P., Heibst, C., Lamon, J., "Determination of Fracture Toughness in 2D Woven SiC Matrix Composites Made By Chemical Vapor Infiltration", J. Am. Ceram. Soc., Vol. 78, No. 5, 1995, pp. 1201-1211.

9. Bikok, M., "Elaboration, Mechanical and Physical Characterization of SiC/SiC Minicomposites, Internal Report (in French) LCTS, 1998.

10. Shiwa, M., Chen, O. Y., Carpenter, S. H., Kishi, T., Mitsuno, S., Ichikawa, H., Lee, Y. T., Kim, S. T., Lee, T. S., "Fracture Mechanisms of SiC/SiC Composite by Means of Acoustic Emission Analysis", J. Jap. Inst. Met., Vol. 59, No. 6, 1995, pp. 627-633.

11. Lissart, N., Lamon, J., "Damage and Fracture in Ceramic Matrix Composites: Experimental Study and Model", Acta Mat., Vol. 15, No. 3, 1997, pp. 1025-1044.